Sentinel-1 Image Classification Using Machine Learning Algorithms Based on the Support Vector Machine and Random Forest

Jamali, A.
Faculty of Surveying Engineering, Apadana Institute of Higher Education, Shiraz, Iran
E-mail: ali.jamali.65@gmail.com

Abstract
Due to concerns of recent earth climate changes such as an increase of earth surface temperature and monitoring its effect on the earth's surface, environmental monitoring is a necessity. Environmental change monitoring in earth sciences needs land use land cover change (LULCC) modeling to investigate the impact of climate change phenomena such as droughts and floods on earth surface land cover. As land cover has a direct effect on Land Surface Temperature (LST), the Land cover mapping is an essential part of climate change modeling. In this paper, for land use land cover mapping (LULCM), image classification of Sentinel-1A Synthetic Aperture Radar (SAR) Ground Range Detected (GRD) data using two machine learning algorithms including Support Vector Machine (SVM) and Random Forest (RF) are implemented in R programming language and compared in terms of overall accuracy for image classification. With seven different scenarios defined in this research, RF and SVM classification methods show their best performance with overall accuracies of 75.30 and 75.35 percent, respectively.

1. Introduction

Land cover is a fundamental factor that links and affects many parts of the human and physical environment (Foody, 2002). The change in land cover is considered as an important factor of global change affecting ecological systems (Vitousek, 1994) with an impact on the earth that is linked with climatic change (Skole, 1994). Land cover mapping (Grippa et al., 2018) and monitoring are some of the key applications of earth observation satellite sensor data, which is an important factor in assessing the results of climate change in the recent years. On the other hand, changes in land cover affect the climate through changes in the composition of greenhouse gasses such as carbon dioxide (Betts et al., 2007; Bonan, 2008 and Bala et al., 2007). Up to date, land use land cover (LULC) statistics are a need for policy and decision making, which has an effect on the economy and society (Costa et al., 2018). According to Rodriguez-Galiano et al. (2012), there are several issues for extensive area land cover monitoring, including:

1. First, complex landscapes are difficult to monitor due to sudden changes in environmental gradients (e.g., moisture, elevation, and temperature) and a legacy of past interference (Rogan and Miller, 2006). Such heterogeneous landscapes are defined by land-cover categories that are complicated to be defined spectrally due to low inter-class separability and high intra-class variability.

2. Second, there is a need for algorithms that can be interpreted readily and automated as well as to be easily run with user-defined parameters that are simple to adjust.

3. Third, a promising land-cover classification algorithm for large area mapping relies on the capability of the algorithm to work with noisy observations, a complex measurement space, and a few numbers of training data compared to the size of the study area (DeFries and Chan, 2000 and Rogan et al., 2008).

A wide range of classification methods has been utilized to map land cover using remotely sensed data. Classification methods vary from unsupervised algorithms such as K-means clustering to supervised parametric algorithms such as maximum likelihood (Otukei and Blaschke, 2010); to machine learning algorithms such as artificial neural networks (Duro et al., 2012), SVMs (Mountrakis et al., 2011; Jamali, 2019a), decision trees (Breiman, 1984 and Hua et al., 2017; Jamali, 2019b), and ensembles of classifiers (Breiman, 1996). The usual purpose of land cover classification is to produce a thematic map of the land cover. Land cover is the material at

the ground, such as vegetation, water, soil, and man-made structures. (Fisher and Unwin, 2005). The number and kind of land cover classes in the image that can be defined vary significantly depending on the sensor resolutions. For land monitoring of forests, water, soil, agriculture, emergency mapping support for natural disasters including flooding, landslide, earthquakes, Sentinel-1A/1B satellites were launched. Sentinel-1 satellites carry a C-SAR sensor, which has medium and high-resolution imaging in all-weather conditions. The C-SAR can obtain night imagery and detecting small movement on the ground, which makes it useful for land and sea monitoring. SAR is known for its day-and-night and all-weather imaging ability.

In last two decades, for SAR image interpretation, several methods including statistical-based (Tison et al., 2004 and Marques et al., 2012), texture-based (Haralick and Shanmugam, 1973 and Torres-Torriti and Jouan, 2001) and model-based (Li, 2009 and Lafferty et al., 2001) methods have introduced (He et al., 2017). A SAR signal has phase and amplitude information where the phase is the fraction of one complete sine wave cycle, and the amplitude is the strength of the radar response. The phase of the SAR image is determined by the distance between the ground targets and the satellite antenna. According to the European Space Agency (ESA), Sentinel-1 can simultaneously collect several different images from the same series of pulses by using its antenna to receive specific polarisations. Basically, Sentinel-1 is a phase-preserving dual-polarization SAR system. It can transmit a signal in both horizontal (H) and vertical (V) polarization and then receive in both H and V polarisations. Dual polarisation Level-1 Single Look Complex (SLC) products contain complex values. In addition to the backscatter intensity that can be measured from every single polarisation, the inter-channel phase information allows performing enhanced analysis of backscattering properties.

In this research, for Sentinel-1A image classification, Random Forest (RF) and Support Vector Machine (SVM) algorithms are implemented in the R programming language and compared in terms of overall accuracy for image classification. Following this introduction, in Section 2, classification methods are discussed. Study area and data used in this research are discussed in Section 3. Results of image classification based on the RF and SVM are presented in Section 4. In Section 5, the results of RF and SVM for image classification are evaluated in terms of overall accuracy. Discussions and conclusions are presented in Section 6.

2. Methods

Two machine learning classification methods, including RF and SVM in R programming language, are researched. For large and complex datasets, machine learning algorithms are more accurate and efficient compared to conventional parametric algorithms (Rodriguez-Galiano et al., 2012). Both RF and SVM are state-of-the-art machine learning algorithms for image classification. RF (Breiman, 2001) method is an extension of classification and regression trees (CART; Breiman et al., 1984). RF method is an ensemble learning technique that is increasingly used in land-cover classification using multispectral and hyperspectral satellite sensor imagery. RF creates several trees based on random bootstrapped of the training dataset samples. RF runs random binary trees that creates a subset of the training over bootstrapping method, from the initial dataset, a random selection of the training data is selected and implemented to construct the model, out of the bag (OOB) is the data which is not included (Catani et al., 2013). The number of trees (ntree), and the number of variables (mtry) are two parameters which are needed to be tuned in an RF method.

SVMs (Vapnik, 1998) uses a simple linear method to the data, but in a high-dimensional feature space non-linearly related to the input space, but in practice, it does not use any computations in that high-dimensional space. The combined state-of-the-art performance and simplicity on many learning problems (regression and classification) have increased the popularity of the SVMs (Leo et al., 2006). SVM is a supervised machine learning technique that is implemented based on the Structural Risk Minimization (SRM) principle and statistical learning theory (Tehrany et al., 2015). SVMs have higher accuracies compared with the traditional approaches, but the results rely on the kernel used, choice of parameters for the chosen kernel, and the method used to generated SVM (Huang et al., 2002).

2. Study Area and Data Used

The data is from Sentinel-1A GRD data belonging to the 15th November 2018 data set of Shiraz city in WGS 84 / UTM zone 39N (see Figure 1). Shiraz is located in the south of Iran, which is built in a green plain at the foot of the Zagros Mountains, 1,500 meters (4,900 feet) above sea level. For Sentinel-1A image classification, seven scenarios with different polarization data combinations are used (see Table 1). The study area is affected by the recent climate change phenomena (i.e., droughts) where it has a considerable number of gardens due to clime change (i.e., droughts) and population growth in the city,

many of these gardens may be lost for new urban city developments. Although the Municipality has taken some measures to preserve these gardens, land cover monitoring is a key factor to monitor the preservation of garden regions over time.

3. Results

3.1 Pre-processing

For this study, Sentinel-1A GRD data is selected due to its high spatial resolutions of 20*22 meters with a pixel spacing of 10*10 meters and the fact that these data are free of charge which make them a valuable data source for researchers and academia working on effects of climate change phenomena on LULC mapping. Zhou et al., (2016) proposed state of the art for image classification method of polarimetric SAR image classification using deep convolutional neural networks and its advantages over conventional image classification methods wherein this research for image classification, two states of the art machine learning algorithms (i.e., RF and SVM) are used and compared in terms of overall accuracy. The presented methods in this research investigate the application and capabilities of machine learning algorithms for Sentinel-1A GRD image classification based on different bands and a combination of them for land use land cover mapping. Sentinel-1A/1B SAR images are required to be pre-processed before any image classification. In this research, using Sentinel Application Platform (SNAP) software, for image pre-processing, a graph is created in GraphBuilder as follows (see Figure 2). In the first step, the orbit state vector is redefined with a polynomial degree of three as metadata of a SAR product are generally not accurate and can be corrected with the precise orbit files which are available days-to-weeks after the generation of the product. In the second step, produces level-1 images are required to be radiometrically corrected because they do not include radiometric corrections, and significant radiometric bias remains. The radiometric correction is necessary for the pixel values to truly represent the radar backscatter of the reflecting surface.

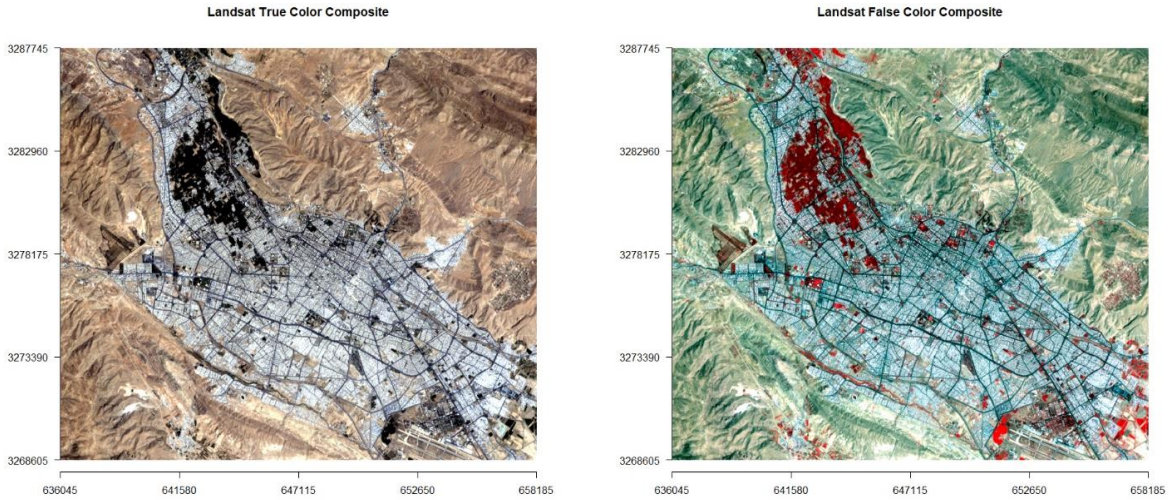

Figure 1: Study area

Figure 2: The implemented pre-processing graph of Sentinel-1A in SNAP

Table 1: The dataset of experiments for land cover classification

Scenario	Number of variables	Variables
1	1	(VV+VH)/2
2	2	VV, VH
3	3	VV, VH, (VV+VH)
4	3	VV, VH, (VV-VH)
5	3	VV, VH, (VV/VH)
6	3	VV, VH, NDDPI
7	4	VV, VH, (VV+VH), (VV-VH)

In the third step, speckles that are caused by random constructive and destructive interference of the de-phased but coherent return waves scattered by the elementary scatter within each resolution cell are filtered with Lee Sigma with a window size of 7by7, sigma of 0.9 and target window size of 3by3. In the final step, for ellipsoidal correction of the Sentinel-1A SAR image, Geo-location Grid is used (see Figure 3).

3.2 Image Classification

Most of the classification methods take a formula such as $Y=X_1+X_2$, to find dependent and independent variables where Y is a function of X_1 and X_2. Considering VV and VH polarimetry data (see Figure 4) plus dual-polarization ratio, dual-polarization difference and dual-polarization multiple for Sentinel-1A GRD data, in R programming language, the classification formula is written by (see Equation 1):

classes ~ (VV)+ (VH) + (VV/VH) + (VV+VH) + (VV-VH) + (NDDPI) + (abs (VV*VH)) (1)

where:

$$Normalized\ Difference\ Dual\ Polarization\ Index = \text{NDDPI} = \frac{VV - VH}{VV + VH}$$

Sentinel-1A images are classified by five materials, including the build-up, soil, water, and vegetation regions, to evaluate the performance of two image classification methods, including RF (see Figure 5) and SVM (see Figure 6) algorithms.

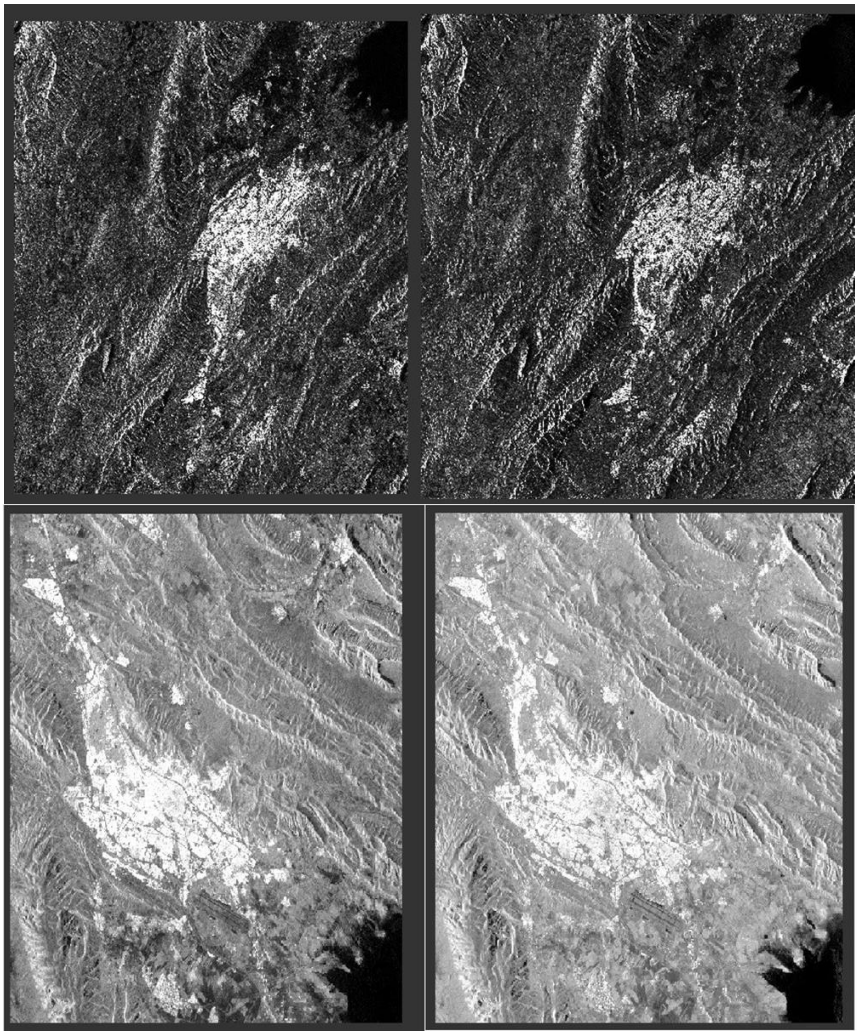

Figure 3: a) Intensity_VH polarization data (top left) b) Intensity_VV polarization data (top right) c) Saigma_0_VH_db polarization data (down left) d) Saigma_0_VV_db polarization data (down right)

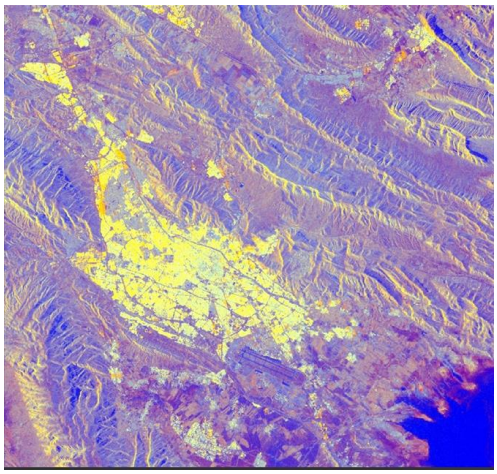

Figure 4: Dual Polarization ratio of VV+ VH of Shiraz city

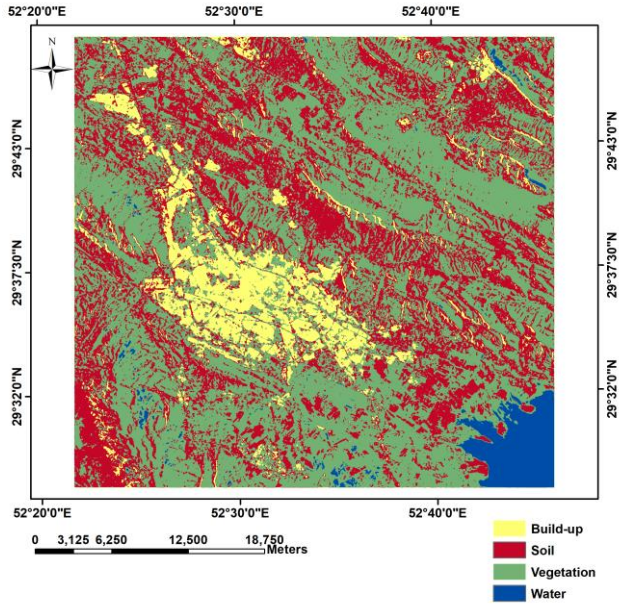

Figure 5: Image classification using Random Forests classification technique within R programming language in scenario 7.

Table 2: Accuracy of predicted materials by RF classification technique in scenario 7.

RF	Build-up	Soil	Vegetation	Water
Build-up	208	0	0	0
Soil	0	11083	369	0
Vegetation	0	8309	1213	0
Water	0	0	0	13617
Overall accuracy	**75.06**			

4. Results Evaluation

To validate the results of image classification techniques, the overall accuracy (see Equation 1) of both RF and SVM algorithms are presented in Tables 2 to 4. RF and SVM classification methods show their best performance with overall accuracies of 75.30 and 75.35 percent respectively for the evaluation dataset in scenarios 5 and 7, respectively.

$$OA = \frac{number\ of\ correctly\ classified\ values}{total\ number\ of\ reference\ values}$$

Equation 1

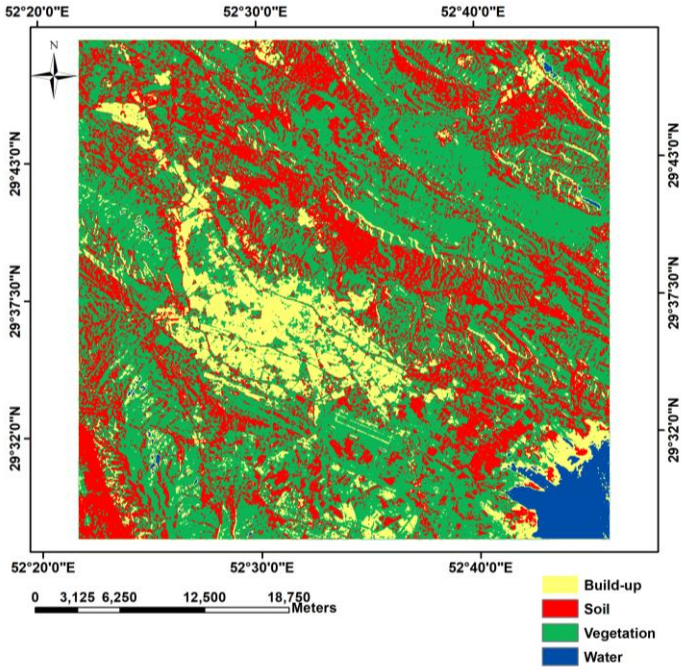

Figure 6: Image classification using SVM classification technique within the R programming language in scenario 7

Table 3: Accuracy% of predicted materials by SVM classification technique in scenario 7

SVM	Build-up	Soil	Vegetation	Water
Build-up	208	0	0	0
Soil	0	11160	345	0
Vegetation	0	8232	1237	0
Water	0	0	0	13617
Overall accuracy	**75.35**			

Table 4: Overall accuracy of FR and SVM image classification methods in seven defined scenarios as defined in Table 1 (in percent)

Scenario	**1**	**2**	**3**	**4**	**5**	**6**	**7**
RF overall accuracy	71.11	74.82	75.13	75.13	75.30	75.16	75.06
SVM overall accuracy	73.94	75.12	74.81	75.35	74.93	74.86	75.35

With seven different scenarios with different defined dual-polarization data information, the RF algorithm has its best performance in scenario 4 with VV, VH, (VV-VH) polarization data. On the other hand, the SVM algorithm shows its best performance in scenario three, which has VV, VH, (VV+VH) polarization information (see Table 4).

5. Discussion and Conclusion

Free and commercial Earth Observation (EO) satellite sensor data are a key factor for large area environmental monitoring. Due to several climate change phenomena (e.g., increase of temperature due to greenhouse gasses) in recent years and their impact on the land cover change and vice versa, the effect of land cover changes on earth climate, image classification for large area environments is a necessity. There are several statistical and mathematical image classification algorithms where in this research performance of two machine learning algorithms for a dataset of Shiraz city in Iran in seven different scenarios (see Table 1) are researched. There are several issues and remarks encountered in this research, as follows:

1. The kernel used in SVM classification technique has four types of linear $'v$, polynomial $(\gamma u'v + coef0)^{degree}$, radial basis function $\exp(-\gamma|u-v|^2)$ and sigmoid $tanh(\gamma u'v + coef0)$. Cost of constraints violation is the constant of the regularization term in the Lagrange formulation, and gamma is a parameter needed for all kernels except linear, which is by default equal to 1/ (data dimension).

The error of image classification based on the RBF SVM for several costs and gammas is presented in Table 5, where the best performance is in cost 100 and gamma 1.

2. SVM algorithm has better overall accuracy for Sentinel-1A GRD data image classification over RF algorithm for the dataset used in this research.

3. Image classification using the SVM algorithm is quite more time consuming compared to the RF algorithm. For the dataset used in this research, the RF method is almost five times faster than the SVM method.

Table 5: Performance of RBF SVM for different gamma and cost parameters

Cost	Gamma	Error
0.1	0.5	0.044
1	0.5	0.040
10	0.5	0.038
100	0.5	0.037
0.1	1	0.041
1	1	0.038
10	1	0.037
100	1	0.036
0.1	2	0.0388
1	2	0.0374
10	2	0.0369
100	2	0.0371

The presented methods can be utilized for feature extraction, recognition, and mappings such as build-up, vegetation regions to be used for time-series land use land cover change mapping due to the effects of human activities or global change, including droughts and floods. Another direct use of the presented methods would be in disaster area mapping, such as flood mapping, where water regions are required to be extracted and recognized from other non-water areas. A fusion of optical and SAR sensors, including Sentinel-1 and Sentinel-2 images for better image classification and combining machine learning algorithms, would be recommended for future research.

References

Bala, G., Caldeira, K., Wickett, M., Phillips, T., Lobell, D., Delire, C. and Mirin, A., 2007, Combined Climate and Carbon-Cycle Effects of Large-Scale Deforestation. *Proceedings of the National Academy of Sciences*, Vol. 104(16), 6550-6555.

Betts, R., Falloon, P., Goldewijk, K. and Ramankutty, N., 2007, Biogeophysical Effects of Land Use on Climate: Model Simulations of Radiative Forcing and Large-Scale Temperature Change. *Agricultural and Forest Meteorology*, Vool. 142 (2-4), 216-233.

Bonan, G., 2008, Forests and Climate Change: Forcings, Feedbacks, and the Climate Benefits of Forests. *Science*, Vol. 320(5882), 1444-1449.

Breiman, L., 1984, Classification and Regression Trees. Chapman & Hall/CRC.

Breiman, L., 1996, Bagging Predictors. *Machine Learning*, Vol. 24(2), 123-140.

Breiman, L., 2001, Random Forests. *Machine Learning*, Vol. 45(1), 5-32.

Catani, F., Lagomarsino, D., Segoni, S. and Tofani, V., 2013, Landslide Susceptibility Estimation by Random Forests Technique: Sensitivity and Scaling Issues. *Nat Hazards Earth Syst Sci*, Vol. 13, 2815-2831.

Costa, H., Almeida, D., Vala, F., Marcelino, F. and Caetano, M., 2018, Land Cover Mapping From Remotely Sensed and Auxiliary Data for Harmonized Official Statistics. *ISPRS International Journal of Geo-Information*, Vol. 7(4), 1-21. DOI: 10.3390/ijgi7040157.

DeFries, R. S. and Chan, J. C. W., 2000, Multiple Criteria for Evaluating Machine Learning Algorithms for Land Cover Classification from Satellite Data. *Remote Sensing of Environment*, Vol. 74(3), 503-515.

Duro, D. C., Franklin, S. E. and Dubé, M. G., 2012, A Comparison of Pixel-Based and Object-Based Image Analysis with Selected Machine Learning Algorithms for the Classification of Agricultural Landscapes using SPOT-5 HRG Imagery. *Remote Sensing of Environment*, Vol. 118, 259-272.

Fisher, P. F. and Unwin, D. J., eds., 2005, Representing GIS. Chichester, England: John Wiley & Sons.

Foody, G. M., 2002, Status of Land Cover Classification Accuracy Assessment. *Remote Sensing of the Environment*, Vol. 80, 185-201.

Grippa, T., Georganos, S., Zarougui, S., Bognounou, P., Diboulo, E., Forget, Y., Lennert, M.,Vanhuysse, S., Mboga, N. and Wolff, E., 2018, Mapping Urban Land Use at Street Block Level Using OpenStreetMap, Remote Sensing Data, and Spatial Metrics. *ISPRS International Journal of Geo-Information*, Vol. *7*(7), 246. https://doi.org/10.3390/ijgi7070246.

Haralick, R. M. and Shanmugam, K., 1973, Textural Features for Image Classification. *IEEE Transactions on Systems, Man, and Cybernetics*,

Vol. SMC-3, No. 6, 610-621. DOI: 10.1109/TSMC.1973.4309314.

He, C., Liu, X., Kang, C., Chen, D. and Liao, M., 2017, Attribute Learning for SAR Image Classification. *ISPRS International Journal of Geo-Information*, Vol. 6(4), 111. https://doi.org-/10.3390/ijgi6040111.

Hua, L., Zhang, X., Chen, X., Yin, K. and Tang, L., 2017, A Feature-Based Approach of Decision Tree Classification to Map Time Series Urban Land Use and Land Cover with Landsat 5 TM and Landsat 8 OLI in a Coastal City, China. *ISPRS International Journal of Geo-Information*, Vol. 6(11), 1-18. DOI: 10.3390/ijgi6110331.

Huang, C., Davis, L.S. and Townshed, J. R. G., 2002, An Assessment Of Support Vector Machines for Land Cover Classification. *International Journal of Remote Sensing*, Vol. 23, 725-749.

Jamali, A., 2019a, a Fit-For Algorithm for Environmental Monitoring Based on Maximum Likelihood, Support Vector Machine and Random Forest. *ISPRS Annals of Photogrammetry, Remote Sensing and Spatial Information Sciences*, 25-32.

Jamali, A., 2019b, Evaluation and comparison of eight machine learning models in land use/land cover mapping using Landsat 8 OLI: a case study of the northern region of Iran. *SN Applied Sciences*, *1*(11), 1448.

Lafferty, J., McCallum, A. and Pereira, F. C., 2001, Conditional Random Fields: Probabilistic Models for Segmenting and Labeling Sequence Data. *Proc. 18th International Conf. on Machine Learning*. 282–289.

Li, S. Z., 2009, *Markov Random Field Modeling in Image Analysis*. Springer Science & Business Media. DOI: 10.1007/978-1-84800-279-1.

Leo, B., Friedman, J. H., Olshen, R. A. and Stone, C. J., 1984, *Classification and Regression Trees*. Wadsworth International Group.

Marques, R. C. P., Medeiros, F. N. and Nobre, J. S., 2012, SAR Image Segmentation Based on Level Set Approach and {\cal G} _A^ 0 Model. *IEEE Transactions on Pattern Analysis and Machine Intelligence*, Vol. 34(10), 2046-2057.

Mountrakis, G., Im, J. and Ogole, C., 2011, Support Vector Machines in Remote Sensing: A Review. *ISPRS Journal of Photogrammetry and Remote Sensing*, Vol. 66(3), 247-259.

Otukei, J. R. and Blaschke, T., 2010, Land Cover Change Assessment Using Decision Trees, Support Vector Machines and Maximum Likelihood Classification Algorithms. *International Journal of Applied Earth Observation and Geoinformation*, Vol. 12, S27-S31.

Rodriguez-Galiano, V. F., Ghimire, B., Rogan, J., Chica-Olmo, M. and Rigol-Sanchez, J. P., 2012, An Assessment of the Effectiveness of a Random Forest Classifier for Land-Cover Classification. *ISPRS Journal of Photogrammetry and Remote Sensing*, Vol. 67, 93-104.

Rogan, J. and Miller, J., 2006, *Integrating GIS and Remotely Sensed Data for Mapping Forest Disturbance and Change. In: Franklin, M.W.A.S. (Ed.), Understanding Forest Disturbance and Spatial Pattern: Remote Sensing and GIS Approaches*. CRC Press, Boca Raton, FL, 133-172.

Rogan, J., Franklin, J., Stow, D., Miller, J., Woodcock, C. and Roberts, D., 2008, Mapping Land-Cover Modifications over Large Areas: A Comparison of Machine Learning Algorithms. *Remote Sensing of Environment*, Vol. 112(5), 2272-2283.

Skole, D. L., 1994, *Data on Global Land Cover Change: Acquisition Assessment and Analysis. In: Turner, II, W.B. (Ed.), Changes in Land Use and Land Cover: A Global Perspective.* Cambridge University Press, Cambridge, 437-471.

Tehrany, M. S., Pradhan, B., Mansor, S. and Ahmad, N., 2015, Flood Susceptibility Assessment using GIS-Based Support Vector Machine Model with Different Kernel Types. *Catena*, Vol. 125, 91-101. doi:10.1016/j.catena-.2014.10.017.

Tison, C., Nicolas, J. M., Tupin, F. and Maître, H., 2004, A New Statistical Model for Markovian Classification of Urban Areas in High-Resolution SAR Images. *IEEE Transactions on Geoscience and Remote Sensing*, Vol. 42(10), 2046-2057.

Torres-Torriti, M. and Jouan, A., 2001, Gabor vs. GMRF Features for SAR Imagery Classification. In *Image Processing, 2001. International Conference* on. Vol. 3, 1043-1046. DOI: 10.1109/ICIP.2001.958305.

Vapnik, V., 1998, *Statistical Learning Theory*. John Wiley&Sons. Inc., New York.

Vitousek, P. M., 1994, Beyond Global Warming: Ecology And Global Change. *Ecology*, Vol. 75, 1861-1876.

Zhou, Y., Wang, H., Xu, F. and Jin, Y. Q., 2016, Polarimetric SAR Image Classification Using Deep Convolutional Neural Networks. *IEEE Geoscience and Remote Sensing Letters*, Vol. 13(12), 1935-1939.